Journal of Quantitative Spectroscopy & Radiative Transfer 111 (2010) 2139–2150

Contents lists available at ScienceDirect

Journal of Quantitative Spectroscopy & Radiative Transfer

journal homepage: www.elsevier.com/locate/jqsrt

HITEMP, the high-temperature molecular spectroscopic database

L.S. Rothman [a,*], I.E. Gordon [a], R.J. Barber [b], H. Dothe [c], R.R. Gamache [d], A. Goldman [e], V.I. Perevalov [f], S.A. Tashkun [f], J. Tennyson [b]

[a] Harvard-Smithsonian Center for Astrophysics, Atomic and Molecular Physics Division, Cambridge MA 02138, USA
[b] Department of Physics and Astronomy, University College London, London WC1E 6BT, UK
[c] Spectral Sciences, Inc., Burlington MA 01803, USA
[d] University of Massachusetts School of Marine Sciences, Department of Environmental, Earth, and Atmospheric Sciences, Lowell MA 01854, USA
[e] University of Denver, Department of Physics, Denver CO 80208, USA
[f] Institute of Atmospheric Optics, Siberian Branch, Russian Academy of Sciences, Tomsk 634055, Russia

ARTICLE INFO

Keywords:
Spectroscopic database
Molecular spectroscopy
Molecular absorption
Line parameters
High-temperature spectroscopy
HITEMP

ABSTRACT

A new molecular spectroscopic database for high-temperature modeling of the spectra of molecules in the gas phase is described. This database, called HITEMP, is analogous to the HITRAN database but encompasses many more bands and transitions than HITRAN for the absorbers H_2O, CO_2, CO, NO, and OH. HITEMP provides users with a powerful tool for a great many applications: astrophysics, planetary and stellar atmospheres, industrial processes, surveillance, non-local thermodynamic equilibrium problems, and investigating molecular interactions, to name a few. The sources and implementation of the spectroscopic parameters incorporated into HITEMP are discussed.

1. Introduction

In the second half of the twentieth century, the simultaneous development of computers, high-resolution laboratory spectroscopy, and sensitive detectors for field instruments led to the establishment of a computer-readable archive of spectroscopic parameters applicable for atmospheric transmission and radiance calculations [1]. The standard database for this work is the HITRAN database [2], which is periodically updated and expanded. HITRAN has its origins in applications for conditions of the terrestrial atmosphere, particularly temperatures ranging from the surface of the Earth to the stratosphere. As a result, there are many molecular bands and line transitions that would be significant at high temperatures that have not necessarily been considered for the HITRAN archive. In addition, there are numerous molecular bands, especially in the near-IR and visible spectral regions, that are still missing from HITRAN due to the lack of either experimental data or theoretical calculations of these lines.

The HITRAN database, used as input to various high-resolution transmission codes, has been successful for a vast number of applications. The foremost application is remote-sensing of the terrestrial atmosphere from spectrometers aboard satellites, balloons, and ground-based instrumentation. There are also environmental, industrial, surveillance problems, and numerous other applications. Industrial, environmental, and surveillance applications often require a high-temperature spectroscopic database. However, the use of HITRAN (established at a reference temperature of 296 K) is usually deficient when applied to problems where gases are at elevated temperatures. There is also the obvious requirement in astrophysics to characterize stellar, brown dwarfs, and planetary atmospheres. For example, the recent detection [3] of water in extrasolar planet HD189733b relied heavily on the BT2 line list [4], which is used in the present work as

* Corresponding author. Tel.: +1 617 495 7474; fax: +1 617 496 7519.
E-mail address: LRothman@cfa.harvard.edu (L.S. Rothman).

0022-4073/$ - see front matter © 2010 Elsevier Ltd. All rights reserved.
doi:10.1016/j.jqsrt.2010.05.001

explained below. The analysis would not have been possible with HITRAN nor reliable with the earlier version of the high-temperature analog [5] to HITRAN. The need for a high-temperature database embraces, for example, some planetary atmospheres such as possessed by Venus or many exosolar planets. An example of the inability of HITRAN to adequately characterize the Venus night-side atmosphere was given in Pollack et al. [6]. In addition, having a database with excited energy levels satisfies the requirements of some non-local thermodynamic equilibrium (NLTE) problems in the atmosphere. A typical example is the Meinel bands [7] of OH, which require transitions between very high energy levels that would not be necessary in normal radiative-transfer applications.

Early attempts to produce a high-temperature database simply scaled the HITRAN database to estimate the absorption and emission spectra at elevated temperatures. In the database, the intensity[1] of a line transition S_{jf} between lower state i and upper state f as a function of temperature T is given by

$$S_{if}(T) = S_{if}(T_{ref})\frac{Q(T_{ref})}{Q(T)}\frac{\exp(-c_2E_i/T)}{\exp(-c_2E_i/T_{ref})}\frac{1-\exp(-c_2\nu_{if}/T)}{1-\exp(-c_2\nu_{if}/T_{ref})}, \quad (1)$$

where T_{ref} is the reference temperature of the database (296 K), Q is the total partition sum, E_i is the energy of the lower state (cm^{-1}), and ν_{if} is the energy difference between the initial and final state (given as vacuum wavenumber, cm^{-1}, in the database). The constant c_2 is the second radiation constant ($c_2=hc/k=1.43877$ cm K). The quantities in Eq. (1) are all provided in the HITRAN compilation. Although the scaling from room temperature to higher temperatures is sufficiently accurate to estimate the line intensity at higher temperature provided an adequate high-temperature partition function is available, the additional spectral lines that are missing from the simulation often lead to a significant underestimation of the source radiance in specific spectral regions.

To address these issues, an analogous database to HITRAN was established and called HITEMP [5] (hereafter called HITEMP1995 to distinguish it from the current effort). This first edition included only the gases H_2O, CO_2, CO, and OH. The water-vapor line parameters were the result of a calculation using the direct numerical diagonalization (DND) method [8] and were aimed at being sufficient for 1000 K. There was also a calculation for 1500 K, but with a limited dynamic range of intensities. The carbon dioxide parameters were also the result of the same theoretical methodology [8], applicable at 1000 K. The carbon monoxide line list was adapted from the work of Goorvitch [9] that was constructed for a solar atlas. Finally, the hydroxyl line list [10] was added to HITEMP1995 since an extensive list was available in HITRAN itself for NLTE applications.

One desirable feature in creating the HITEMP database (hereafter called HITEMP2010 when referring to the new edition) is to have it consistent with the HITRAN database. That is, it is preferable to have any transitions in common be identical since some simulations might use HITEMP for the source with HITRAN representing the intervening atmospheric path. Having this correlation of lines was simple for CO and OH, where the HITRAN and HITEMP line lists for these gases were generated from the common sources. For CO_2, constraints were applied that heavily weighted the molecular constants in the fit to the HITRAN values. However, for H_2O the problem was much more complicated since the data in HITRAN consist of many different contributions, both experimental and calculated, and from different sources. Thus common lines found in HITEMP1995 were superseded by their counterpart in HITRAN (the edition of the HITRAN database [11] at that time). This method relies on the quantum identifications of transitions in both databases being consistent, by no means assured, especially for the higher polyads. This method can also introduce discontinuities in the line positions of bands as one migrates to higher rotational values.

With these limitations of the older version, HITEMP1995, in mind, and with new calculations and experiments that have become available, we embarked on a program [12] to substantially update the database, as described in the following sections.

2. Structure of the database

The format of HITEMP2010 has been maintained to be the same as that of HITRAN. Thus, the HITEMP1995 edition [5] had the 100-character length transition record that was established in 1986 [13]. The current HITRAN edition has increased the length of each transition to 160 characters. Table 1 gives a description of the current list of parameters, definition of units, and format. The databases are in ASCII files and, while following the HITRAN format makes the HITEMP2010 database quite large, it was chosen to make it easily compatible to the same programs that make use of HITRAN.

Similarly, the intensity is given at the HITRAN standard temperature of 296 K, even though calculations have been performed at much higher temperatures. Usage of the database requires converting by Eq. (1) back to the temperature of the application, which is done routinely in transmission or radiance codes. The standardization to 296 K means that some of the intensities in the database may have very low exponents and require double precision when being used.

One of the most difficult entities to define for the archival databases is the criterion for the cutoff in intensities. This lower limit for intensities had some physical meaning for the uniformly mixed gases in HITRAN, i.e., to include all lines that contributed at least a 10% absorption over a maximal path in the terrestrial atmosphere, namely space to space tangent to the surface.

[1] The units adopted for the parameters in the molecular spectroscopic databases are the cgs system. The units of intensity are given in wavenumber per column density, cm^{-1}/(molecule cm^{-2}), which can be simplified to cm $molecule^{-1}$ although this form obscures the origin. Note also that we employ the symbol ν throughout for line position in cm^{-1}, thereby dropping the tilde ($\tilde{\nu}$) that is the official designation of wavenumber.

Table 1
Description of the parameters and format of the current HITRAN and HITEMP databases.

Symbol	Parameter	Field length	Data type	Comments or units
M	molecule number	2	Integer	HITRAN chronological assignment
I	isotopologue number	1	Integer	Ordering by terrestrial abundance
v	Vacuum wavenumber	12	Real	cm^{-1}
S	Intensity	10	Real	$cm^{-1}/(molecule \times cm^{-2})$ at standard 296 K
A	Einstein A-coefficient	10	Real	s^{-1}
γ_{air}	Air-broadened halfwidth	5	Real	HWHM at 296 K (in cm^{-1} atm^{-1})
γ_{self}	Self-broadened halfwidth	5	Real	HWHM at 296 K (in cm^{-1} atm^{-1})
E''	Lower-state energy	10	Real	cm^{-1}
n	Temperature-dependence coefficient	4	Real	Temperature-dependent exponent for γ_{air}
δ	Air-pressure-induced line shift	8	Real	cm^{-1} atm^{-1} at 296 K
V'	Upper-state "global" quanta	15	Text	see Table 3 of Ref. [14]
V''	Lower-state "global" quanta	15	Text	see Table 3 of Ref. [14]
q'	Upper-state "local" quanta	15	Text	see Table 4 of Ref. [14]
Q''	Lower-state "local" quanta	15	Text	see Table 4 of Ref. [14]
I_{err}	Uncertainty indices	6	Integer	Uncertainty indices for 6 critical parameters (v, S, γ_{air}, γ_{self}, n, δ)
I_{ref}	Reference indices	12	Integer	Reference pointers for 6 critical parameters (v, S, γ_{air}, γ_{self}, n, δ)
*	Flag	1	Text	Pointer to program and data for the case of line mixing
g'	Statistical weight of the upper state	7	Real	See details in Ref. [15]
g''	Statistical weight of the lower state	7	Real	See details in Ref. [15]

Table 2
High-temperature water-vapor line lists.

Line list	Potential-energy surface	Dipole-moment surface	Spectral range (cm^{-1})	Number of transitions
HITEMP1995 Ref. [5]	Fitted Ref. [8]	Fitted Ref. [8]	0–24,900	1,283,466
AMES Ref. [16]	Fitted Ref. [16]	ab initio Ref. [17]	0–25,000	$\sim 3.08 \times 10^8$
SCAN Ref. [18]	Fitted Ref. [19]	ab initio Ref. [20]	450–30,000	$\sim 3 \times 10^9$ ($\sim 1 \times 10^8$ in reduced format)
BT2 [4]	Fitted Ref. [21]	ab initio adjusted from Ref. [17]	0–30,000	$\sim 5.06 \times 10^8$

The ability to accurately calculate or measure weak lines has improved over time, and this criterion has been relaxed in HITRAN to include weaker lines. However, numerous groups have applied different constraints on the construction of line lists. With calculations it is often simply a maximum rotational quantum number that is chosen, since at higher values the energy expressions may be too expensive to calculate using variational methods or they may be divergent using perturbation theory. The earlier edition, HITEMP1995, employed a rationale of scaling the cutoff in intensities by the Boltzmann distribution at the different temperatures of 1000 and 296 K for water vapor and carbon dioxide, respectively. Other groups have limited their line lists based on experimental limitations such as detector response, optical properties of absorption cells, etc. The cutoff criteria of the intensities for the molecules in HITEMP2010 are discussed in the following section.

3. Components of HITEMP

3.1. H_2O

For the HITEMP1995 water vapor line list a cutoff in intensities of 3.7×10^{-27} cm molecule^{-1} at 1000 K was employed. This cutoff has significantly reduced the capabilities of HITEMP1995 to accurately predict spectra above 1000 K, although it has been fairly accurate for temperatures below and around 1000 K. Taking into account that the potential-energy surface (PES) and dipole moment surface (DMS) used for the generation of HITEMP1995 are now considered outdated, there is an obvious need of creating a new HITEMP database.

The purpose of this work is to provide a compilation of the best available experimental and theoretical data for hot water vapor that would provide accurate simulations of spectra for temperatures up to 4000 K. A number of new theoretical line lists have emerged over the last decade. The most extensive theoretical datasets, along with sources for the PES and DMS used for their generation, spectral ranges, and number of lines are given in Table 2.

The BT2 line list has been extensively used, and in a number of cases has been subjected to comparative studies, with other available line lists. In particular Campargue et al. [22] found that it accurately predicted weak water spectra in the 770 nm transparency window; Bailey [23] strongly recommended it for use in models of the Venus atmosphere, and Kranendonk et al. [24] found that its use allowed them to perform thermometry in flames up to 2000 K with greatly improved reliability. All these works give comparisons with model spectra generated using BT2. We have compared the BT2 dataset

with experimental data from Ref. [25], one of the few available laboratory emission spectra of very hot water for which absolute intensities are available.

Fig. 1 shows experimental and synthetic spectra in 1.3–2.3 μm range. The experiment was carried out at 2900 K, and we compared it with the 3000 K synthetic spectra generated using line lists from Table 2. The emission measurements [25] were made with an echellete grating monochromator using InSb or HgCdTe detectors. The average spectral slit widths were 60 and 180 Å for wavelengths $\lambda < 5$ and $\lambda > 5$ μm, respectively. All calculations were performed using a rectangular apparatus function with 2 Å (=2 cm^{-1}) width. It should be stressed that all experimental points shown in Fig. 1 were obtained by digitizing Fig. 2 of Ref. [25]; thus, the accuracy of experimental points is rather low.

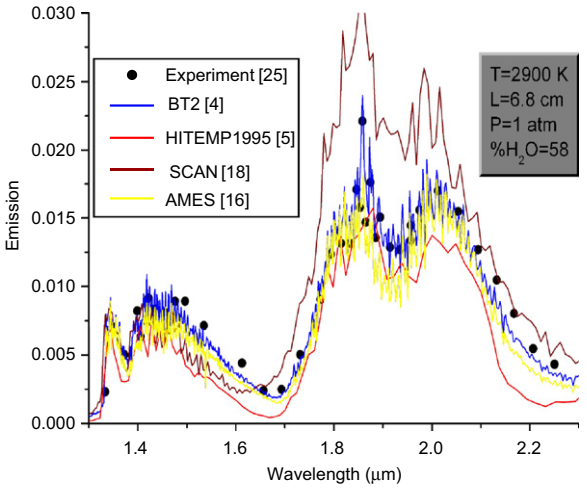

Fig. 1. Comparison of synthetic emission generated using different theoretical water-vapor line lists with high-temperature observations [25]. The reference temperature is 3000 K and the intensity cutoff is 10^{-27} cm molecule^{-1}.

A cutoff of 10^{-27} cm molecule^{-1} was employed for all of the lists in the process of generating this figure. It is clear that the list created by Barber et al. [4], hereafter referred to as BT2, provided the best match with the experimental spectrum. It was chosen to be the starting point for constructing the new HITEMP2010.

The BT2 dataset, along with accompanying software, is capable of generating over 505 million transitions of $H_2^{16}O$ in the 0–30,000 cm^{-1} region with oscillator strengths down to 10^{-36} Debye^2. The only restriction applied in creating the BT2 list was that only rotational levels with $J \leq 50$ were considered. As discussed in the original BT2 paper [4], even at a temperature of 4000 K, the missing levels above J=50 contribute less than 0.02% to the total partition function. Even with this limitation, BT2 cast into the HITRAN2004 format would yield a file as large as 90 Gigabytes, which is not practical for the general use of the database. Therefore it was decided to reduce the number of transitions, but in a way that the database would still be suitable for the majority of high-temperature applications including the most demanding such as non-local thermodynamic equilibrium (NLTE) calculations. A particularly good example is the work on emission spectra from comets where BT2 assigned highly NLTE transitions that had been previously ignored and

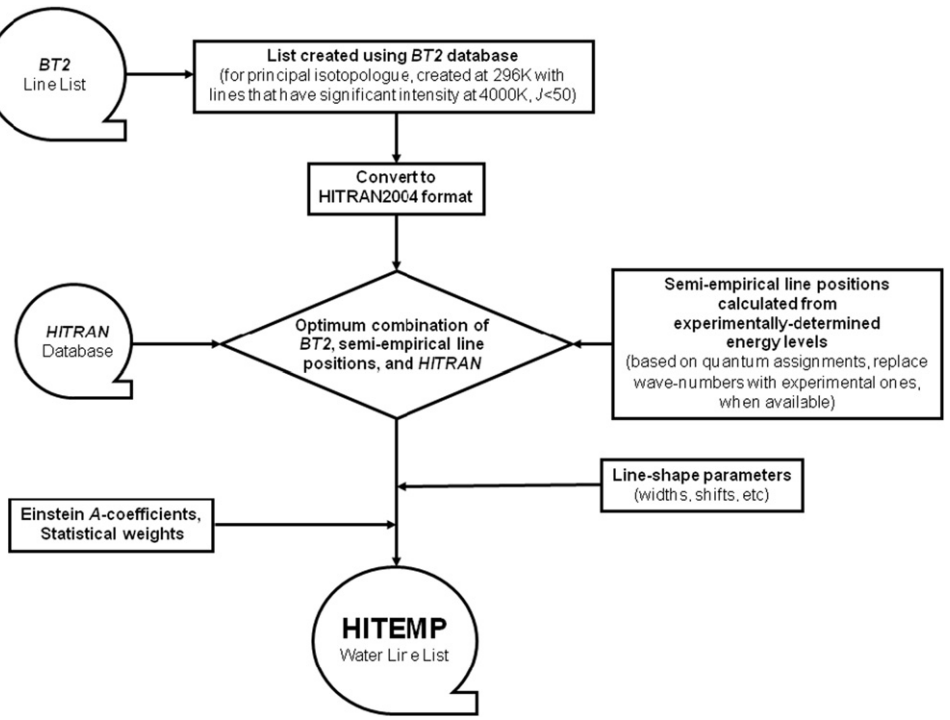

Fig. 2. Flow diagram of water-vapor line list assembly.

which undoubtedly contain new physical insight into the system [26].

The intensity cutoff taken at a certain temperature (as was done in HITEMP1995) is a very coarse approach since the intensity distribution changes with temperature, while it is desired that the database will be suitable over the great range of temperatures. Other approaches for introducing intensity cutoffs to the water-vapor lines exist. For instance, Sharp and Burrows [27] suggested that for calculations of opacities for brown dwarfs and exoplanet atmospheres, lines with $S \geq 10^{-40}$ cm molecule^{-1} at 296 K be considered. Also recently, Perez et al. [28] undertook a similar task for data reduction when they were reducing the amount of lines in the AMES database [16] for plume signature computations. The sophisticated line rejection procedure in that work was performed with a criterion of maximum allowable error on the radiance (ΔI) of the heterogeneous path. ΔI is proportional to the maximum error, $\delta\alpha_k$, in the absorption coefficient in each layer k, and the rejection was carried out in a way that the absorption coefficient due to rejected lines in the layer k is lower than $\delta\alpha_k$. By applying this criterion, which was also temperature dependent, Perez et al. [28] have omitted 95% of the lines from the AMES database in the 600–6000 cm^{-1} region, while still being able to perform their calculations at the desired level of accuracy. However, for this HITEMP database, we have decided to retain a much higher percentage of transitions from the BT2 database since some of the HITEMP users are working on even more extreme applications than plume signatures, such as radiative transfer in stellar atmospheres, for example.

At first, the complete line list at 296 K was generated using BT2 data and the software that accompanies it. The partition function used was that from HITRAN, $Q(296)=174.64$. Then a filtering procedure was applied using the following criteria. The intensity $S(T)$ was evaluated at temperatures from 296 to 4000 K using Eq. (1) in 500 K intervals. At each of the probed temperatures, $S(T)$ is compared with the intensity cutoff $S_{cut}(T)$, defined in three wavenumber domains.

$$S_{cut}(T) = \frac{S_{crit}\nu}{\nu_{crit}} \tanh\left(\frac{c_2\nu}{2T}\right) \quad 0 < \nu \leq 5000\,\mathrm{cm}^{-1}, \tag{2a}$$

$$S_{cut}(T) = S_{crit} \quad 5000 < \nu \leq 7000\,\mathrm{cm}^{-1}, \tag{2b}$$

$$S_{cut}(T) = 1 \times 10^{-27}\,\mathrm{cm\ molecule}^{-1} \quad \nu > 7000\,\mathrm{cm}^{-1}, \tag{2c}$$

where $S_{crit}=3\times10^{-27}$ cm molecule^{-1}, $\nu_{crit}=2000$ cm^{-1}. Eq. (2a) was chosen to account for the radiation field at very low wavenumber. The different criteria for the other wavenumber ranges, Eqs. (2b) and (2c), were simply introduced to permit more lines in the near-IR and visible, which are of course weak, to be retained.

Only those lines with $S(T) > S_{cut}(T)$ at any temperature between 296 and 4000 K were kept for inclusion into HITEMP2010. On average about 25% of the lines that can be generated using BT2 end up being retained using this rejection procedure. The resultant file is then converted to HITRAN2004 format [14] and serves as a base for assembling the new HITEMP2010 compilation.

The next step is achieving consistency with the latest HITRAN water-vapor data, which is the file 01_hit09.par. For that purpose, whenever there is a transition in the filtered BT2 file described above that is also available in HITRAN, it will be removed and replaced with the one in HITRAN with two important exceptions. The first exception is associated with a problem of correspondence of quantum assignments of energy levels between the theoretical BT2 list and the experimental lists. This is due to the fact that only the rotational quantum number J and symmetry can be unambiguously identified using the theoretical potential-energy surface. Different experimental works that contributed to HITRAN have used different potential-energy surfaces to aid in the assignments of the observed transitions, which can occasionally result in ambiguities of quantum assignments. Therefore it was decided to replace a BT2 line with one from HITRAN only if the difference between the line positions in the two datasets is less than 1.5 cm^{-1} when $\nu \leq 5000$ cm^{-1}, 2 cm^{-1} when $5000 < \nu \leq 15{,}000$, and 2.5 cm^{-1} when $\nu > 15{,}000$ cm^{-1}. A second exception is when HITRAN intensities have the reference code 19, which corresponds to experimental intensities of two blended lines combined into one. In this case only the line position is taken from HITRAN, while the BT2 intensity is retained. Since the BT2 list provides data only for the principal isotopologue, the lines for other isotopologues have been taken from HITRAN for the current effort. Future updates will consider high-temperature data for the isotopologues, such as is available in the recent VTT line list for HDO [29].

Finally, we have created a line list (hereafter referred to as the list of semi-empirical line positions or SELP) that contains the transition wavenumbers calculated using the database of experimental energy levels [30] as updated by Zobov using recent high-temperature experiments such as Refs. [31–33]. When possible, the line positions originating from the BT2 database have been replaced with the ones from the SELP list, with the same restrictions that were applied for the introduction of HITRAN line positions. In the future the HITEMP database will benefit from the ongoing International Union of Pure and Applied Chemistry (IUPAC) effort, which includes validating and putting together all available experimentally determined energy levels. This effort has already proved efficient in the case of the $H_2^{18}O$ and $H_2^{17}O$ isotopologues [34].

The flow diagram in Fig. 2 summarizes the procedure of creating the new HITEMP2010 water-vapor line list.

The addition of the collision-induced parameters, namely the air-broadened half-width γ_{air} and its temperature-dependence exponent n, the pressure-induced line shift δ_{air}, and the self-broadened half-width γ_{self}, was accomplished using the slightly extended [2] procedure of Gordon et al. [35], here improved to consider the high rotation–vibration levels now in the HITEMP database. Some problems encountered in this new line list are that the vibrational and rotational quantum numbers are often not fully known, or only partially known. Only a small percentage of transitions taken from the BT2 database has a full description of the quantum numbers (in normal mode representation), i.e. v_1', v_2', v_3', v_1'', v_2'', v_3'', J', K_a, K_c', J'', K_a'', and K_c''. Here, v_1, v_2, and v_3 are the quanta of

vibration for the symmetric stretch, the bending mode, and the antisymmetric stretch, respectively. Single primes denote the upper state, while double primes the lower state. The total angular momentum quanta are given by J, and K_a and K_c are the standard quanta of projection for an asymmetric rotor molecule. Some transitions have either only the rotational quantum numbers, or only J' and symmetry for the upper level and J'', K_a'', and K_c'' for the lower level, or finally J and symmetry for the upper and lower levels.

Thus the algorithm of Gordon et al. [35] must be modified to work correctly for all situations. For $J \leq 25$ and the complete set of quantum assignments, the previous extended algorithm [35] works fine. When the vibrational quantum numbers are not given, the change in vibrational quanta can be estimated by the wavenumber of the transition. For cases with full rotational quantum numbers, approximate values for γ_{air} and δ_{air} can be obtained using the work of Jacquemart et al. [36], which is incorporated into the extended algorithm. Likewise when only the lower state J'', K_a'', K_c'' or only the J'' and symmetry are given, the work of Ref. [36] can be used.

For transitions with $J > 25$ or missing quantum information, we used half-widths averaged for each J'' as discussed below. This option currently exists in the extended algorithm for $J \leq 25$. Because of the nature of the HITEMP database, the method must be extended to $J=50$. We have been able to accomplish this by noting that for water vapor as one goes up in J and K_a the collision process responsible for the broadening goes more and more off-resonance and the half-width goes to a limiting value. For air broadening, both the measurement database [37] and the theoretical calculations for the pure rotation band [38] were investigated. From this analysis, a limiting value of γ_{air} $(J''=50)=0.00839\ \mathrm{cm^{-1}\ atm^{-1}}$ was determined. The rotation band data were then taken and averaged as a function of J''. Because the data at J'' equal to 19 and 20 do not have a complete sampling of transitions, these averages were adjusted to 0.0270 and 0.0240 $\mathrm{cm^{-1}\ atm^{-1}}$, respectively. The points at J'' equal to 49 and 50 were set to the limiting value. The data were then fit to a third order polynomial in J''. The data, averaged as a function of J'', and the polynomial fit are presented in the top panel of Fig. 3. A similar figure was made with the measurement database results, but was not used due to scatter in the measured values.

The above procedure was repeated for self-broadening of water vapor. The measurement database and the calculations made for the 3.2–17.76 μm region [39] were studied giving the self-broadened limiting value of γ_{self} $(J''=50)=0.0400\ \mathrm{cm^{-1}\ atm^{-1}}$. The averages were calculated using the calculated data for the 3.2–17.76 μm region and the value at $J''=18$ was adjusted to $0.1800\ \mathrm{cm^{-1}\ atm^{-1}}$. The points at J'' equal to 49 and 50 were set to the limiting value and these data fit to a third order polynomial in J''. In the lower panel of Fig. 3 the data, the average as a function of J, and the polynomial fit are presented. Again, a similar figure using the measurement database was made, which displayed even more scatter than the air-broadened half-width measurements, so it was not used for the fit.

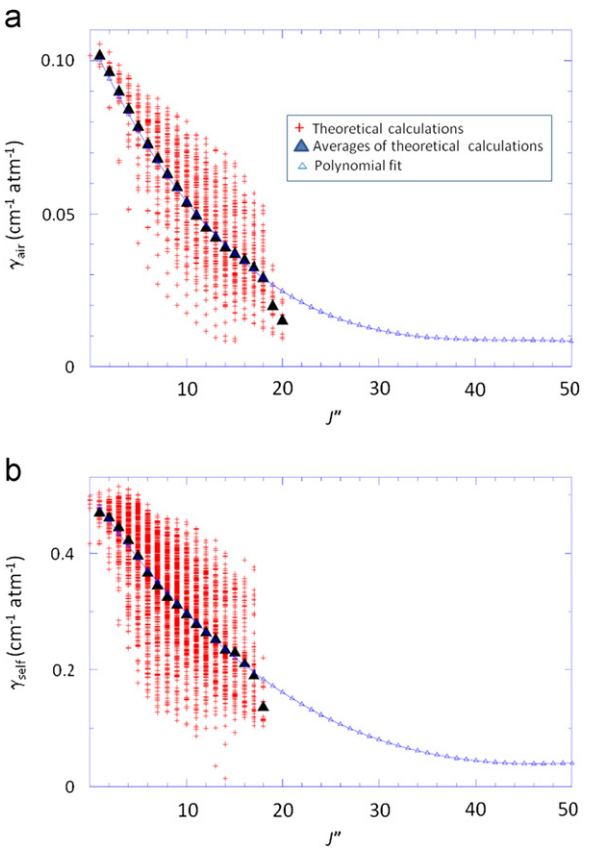

Fig. 3. Extrapolation of average values of (a) air- [38] and (b) self-broadened [39] calculated half-width values as a function of J''.

Table 3
H_2O air- and self-broadened half-widths in $\mathrm{cm^{-1}\ atm^{-1}}$ determined from the polynomial as a function of J''.

J''	γ_{air}	γ_{self}	J''	γ_{air}	γ_{self}
0	0.10691	0.50361	26	0.01546	0.10656
1	0.10035	0.47957	27	0.01441	0.09933
2	0.09409	0.45633	28	0.01347	0.09257
3	0.08812	0.43388	29	0.01265	0.08629
4	0.08244	0.41221	30	0.01193	0.08046
5	0.07703	0.39129	31	0.01130	0.07507
6	0.07190	0.37113	32	0.01076	0.07012
7	0.06703	0.35170	33	0.01031	0.06559
8	0.06242	0.33300	34	0.00992	0.06146
9	0.05806	0.31501	35	0.00961	0.05773
10	0.05395	0.29773	36	0.00936	0.05438
11	0.05007	0.28113	37	0.00916	0.05140
12	0.04642	0.26521	38	0.00901	0.04878
13	0.04299	0.24996	39	0.00890	0.04651
14	0.03978	0.23536	40	0.00882	0.04457
15	0.03677	0.22140	41	0.00876	0.04295
16	0.03397	0.20806	42	0.00873	0.04165
17	0.03136	0.19534	43	0.00870	0.04064
18	0.02894	0.18323	44	0.00868	0.03991
19	0.02670	0.17170	45	0.00866	0.03946
20	0.02463	0.16076	46	0.00863	0.03927
21	0.02273	0.15038	47	0.00858	0.03932
22	0.02098	0.14056	48	0.00851	0.03961
23	0.01939	0.13128	49	0.00841	0.04013
24	0.01795	0.12252	50	0.00827	0.04085
25	0.01664	0.11429			

The final half-widths determined from the polynomial fits of the J''-averaged data are given in Table 3.

The user has to be aware that at high temperatures some of the parameters may be found to be inaccurate. For example, the exponential temperature dependence model used for the air-broadened half-widths given in HITRAN has been shown to be inadequate for many water-vapor transitions and for large temperature ranges [38,40,41].

A sample extract of 41 HITEMP2010 water lines is shown in Fig. 4. The definition of the parameter columns can be ascertained from Table 1. The line in bold font is a transition for which the line position was taken from SELP. The Transition in bold italic is taken from HITRAN2008. All the other lines have wavenumbers and intensities taken from BT2. Whenever a rotational quantum number could not be determined unambiguously, the index of symmetry (1–4 as defined in Ref. [4]) accompanied with a negative sign was used. Note that 1 and 2 indicate para states, whereas 3 and 4 indicate ortho states. For the case of unassigned vibrational quanta, a "−2" label was used.

It is worth noting that if one uses the JavaHAWKS software accompanying the HITRAN compilation to generate the list corresponding to the desired temperature, the partition sums from HITRAN will be automatically employed. These partition sums are available only up to 3000 K, and if one wants to perform calculations for water vapor at higher temperatures, the partitions sums from Vidler and Tennyson [42] that are available up to 6000 K are recommended.

3.2. CO_2

The parameters for carbon dioxide in the HITEMP1995 database were based on the direct numerical diagonalization (DND) [8] calculation. For the line positions, a power series expansion in the product of rotational quantum number, $J(J+1)$, was employed. In the case of well-observed bands, the experimental line positions were heavily weighted and artificial high-J lines were added based on the DND calculation, but with very low weight. In this manner, it was expected to avoid the usual divergence while at the same time maintaining a consistency with HITRAN for common lines. The DND calculations relied ultimately on the experimental dataset being used for the development of the PES and DMS. Comparisons with new observations and with the more recent carbon dioxide spectroscopic database (CDSD-296) [43] have determined that the CDSD database is a clear improvement over the CO_2 data in HITEMP1995.

In the intervening years since the first edition of HITEMP, a high-temperature version of the Carbon Dioxide Spectroscopic Database was developed for 1000 K [44]. This databank included more than 3.6×10^6 lines of four major isotopologues, $^{12}CO_2$, $^{13}CO_2$, $^{16}O^{12}C^{18}O$, and $^{16}O^{12}C^{17}O$ and covered the spectral range from 263 to 9648 cm^{-1}. For CDSD, a cutoff in intensities of 1.0×10^{-27} cm $molecule^{-1}$ at 1000 K was employed. Terrestrial isotopic abundances were used. The databank was extensively tested against measured medium-resolution, high-temperature spectra of pure CO_2 [45] for the 15, 4.3, 2.7, and 2.0 μm bands at temperatures of 1000, 1300, and 1550 K. Good agreement between measured and calculated medium-resolution spectra was found. CDSD was used as a source databank to create high-accuracy, compact databases of narrow-band k-distributions for pure CO_2 [46] and for mixtures of water vapor and carbon dioxide [47]. The databank was also used to verify a multiscale Malkmus model for treatment of inhomogeneous gas paths [48].

```
11 6503.551630 1.425E-36 1.042E-01.07100.371 6968.22250.47-.003644     0 8 0     0 4 0  6  4  3    6  3  4   33223043322571 4 7    39.0   39.0
11 6503.551900 1.969E-50 3.808E-01.01950.13113829.64500.410.000000    -2-2-2    -2-2-2 22 -1 -1   23 -2 -2   13223042329171 2 0    45.0   47.0
11 6503.552100 1.403E-62 2.953E-01.05400.29819374.80740.450.000000    -2-2-2    -2-2-2 10 -1 -1   10 -2 -2   13223042329171 2 0    21.0   21.0
11 6503.552600 3.681E-63 5.466E-01.02670.17219914.46650.410.000000    -2-2-2    -2-2-2 20 -1 -1   19 -2 -2   13223042329171 2 0    41.0   39.0
11 6503.552900 2.210E-70 9.799E-02.01450.09923260.63300.410.000000    -2-2-2    -2-2-2 26 -3 -3   27 -4 -4   13223042329171 2 0   159.0  165.0
11 6503.553700 5.707E-67 4.803E-01.02900.18321682.20160.410.000000    -2-2-2    -2-2-2 19 -2 -2   18 -1 -1   13223042329171 2 0    39.0   37.0
11 6503.553700 3.389E-65 1.995E-01.01950.13120916.66920.410.000000    -2-2-2    -2-2-2 22 -3 -3   23 -4 -4   13223042329171 2 0   135.0  141.0
11 6503.553900 6.120E-62 2.717E-01.01550.10719245.14350.410.000000    -2-2-2    -2-2-2 26 -2 -2   26 -1 -1   13223042329171 2 0    53.0   53.0
11 6503.554100 9.735E-66 1.333E-01.05010.28120969.43520.390.000000    -2-2-2    -2-2-2 12 -3 -3   11 -4 -4   13223042329171 2 0    75.0   69.0
11 6503.554100 1.855E-47 1.072E-01.03400.20812322.22940.380.000000    -2-2-2    -2-2-2 16 -4 -4   16 -3 -3   13223042329171 2 0    99.0   99.0
11 6503.554100 1.761E-63 2.009E-01.02900.18319827.65240.410.000000    -2-2-2    -2-2-2 17 -2 -2   18 -1 -1   13223042329171 2 0    35.0   37.0
11 6503.554200 2.176E-65 4.729E-02.01670.11420737.46270.410.000000    -2-2-2    -2-2-2 25 -4 -4   25 -3 -3   13223042329171 2 0   153.0  153.0
11 6503.554300 1.125E-62 3.231E-01.02670.17219802.43820.410.000000    -2-2-2    -2-2-2 20 -3 -3   19 -4 -4   13223042329171 2 0   123.0  117.0
11 6503.554300 3.531E-70 3.200E-01.04640.26523268.92350.370.000000    -2-2-2    -2-2-2 13 -4 -4   12 -3 -3   13223042329171 2 0    81.0   75.0
11 6503.554400 8.102E-54 1.266E-02.02900.18314929.81020.410.000000    -2-2-2    -2-2-2 19 -3 -3   18 -4 -4   13223042329171 2 0   117.0  111.0
11 6503.554500 4.193E-68 8.534E-01.02280.15022593.05060.410.000000    -2-2-2    -2-2-2 22 -4 -4   21 -3 -3   13223042329171 2 0   135.0  129.0
11 6503.555100 2.981E-55 9.961E-03.02670.17215559.88850.410.000000    -2-2-2    -2-2-2 19 -4 -4   19 -3 -3   13223042329171 2 0   117.0  117.0
11 6503.555300 2.300E-55 5.325E-02.02100.14115761.51750.410.000000    -2-2-2    -2-2-2 22 -2 -2   22 -1 -1   13223042329171 2 0    45.0   45.0
11 6503.555300 1.795E-69 9.524E-01.01950.13123055.38030.410.000000    -2-2-2    -2-2-2 24 -2 -2   23 -1 -1   13223042329171 2 0    49.0   47.0
11 6503.556200 3.681E-68 8.623E-02.01670.11422174.01090.410.000000    -2-2-2    -2-2-2 25 -4 -4   25 -3 -3   13223042329171 2 0   153.0  153.0
11 6503.556300 1.802E-59 6.579E-02.01350.09318031.87140.410.000000    -2-2-2    -2-2-2 29 -3 -3   28 -4 -4   13223042329171 2 0   177.0  171.0
11 6503.556300 2.620E-69 1.324E+00.02900.18322976.10610.410.000000    -2-2-2    -2-2-2 17 -1 -1   18 -2 -2   13223042329171 2 0    35.0   37.0
11 6503.556500 4.697E-69 2.040E-01.04300.25022658.58120.360.000000    -2-2-2    -2-2-2 14 -4 -4   13 -3 -3   13223042329171 2 0    87.0   81.0
11 6503.556860 2.057E-25 2.957E-02.06030.315 1477.29740.30-.014944     1 2 0     0 0 0  8  4  5    9  5  4   35424330182871 4 8    51.0   57.0
11 6503.556900 3.763E-56 1.525E+00.09130.41216441.33320.65-.007980     2 6 2     0 6 2  3  1  3    4  0  4   13223042322571 4 7     7.0    9.0
11 6503.557000 6.594E-60 1.785E-01.06010.33317984.87990.490.000000    -2-2-2     3 2 1  9 -2 -2    8  5  4   13223042329571 2 0    19.0   17.0
11 6503.557000 1.576E-66 1.806E-01.00940.05521395.30460.410.000000    -2-2-2    -2-2-2 35 -1 -1   36 -2 -2   13223042329171 2 0    71.0   73.0
11 6503.557100 1.919E-62 5.677E-02.02280.15019344.59230.410.000000    -2-2-2    -2-2-2 21 -4 -4   21 -3 -3   13223042329171 2 0   129.0  129.0
11 6503.557200 1.885E-66 9.429E-01.03680.22121540.80660.380.000000    -2-2-2    -2-2-2 16 -1 -1   15 -2 -2   13223042329171 2 0    33.0   31.0
11 6503.557200 4.225E-60 2.924E+00.08270.35218854.84170.530.000000    -2-2-2     012 0  8 -4 -4    7  2  5   13223042329571 2 0    51.0   45.0
11 6503.557300 1.515E-69 3.867E-01.06710.35222887.29010.590.000000    -2-2-2    -2-2-2  7 -4 -4    7 -3 -3   13223042329171 2 0    45.0   45.0
11 6503.557600 4.489E-61 1.275E+00.05010.28119207.52400.410.000000    -2-2-2    -2-2-2 11 -4 -4   11 -3 -3   13223042329171 2 0    69.0   69.0
11 6503.557800 1.657E-56 2.583E-01.02470.16116618.22260.410.000000    -2-2-2    -2-2-2 21 -2 -2   20 -1 -1   13223042329171 2 0    43.0   41.0
11 6503.557900 2.217E-43 1.990E-02.02030.183 9830.29930.410.000000    -2-2-2     1 1 0 17 -1 -1   18  5 13   13223042329771 2 0    35.0   37.0
11 6503.558200 4.966E-65 8.454E-01.02670.17221116.00220.410.000000    -2-2-2    -2-2-2 20 -3 -3   19 -4 -4   13223042329171 2 0   123.0  117.0
11 6503.558400 8.523E-52 1.401E+00.01450.09914784.94990.410.000000    -2-2-2     0 0 0 27 -1 -1   27 25  3   13223042329171 2 0    55.0   55.0
11 6503.558400 2.557E-51 1.401E+00.01450.09914784.94990.410.000000    -2-2-2     0 0 0 27 -3 -3   27 25  2   13223042329171 2 0   165.0  165.0
11 6503.558500 1.180E-54 4.021E-01.01950.13115858.59300.410.000000    -2-2-2    -2-2-2 24 -2 -2   23 -1 -1   13223042329171 2 0    49.0   47.0
11 6503.559300 1.951E-41 2.849E-02.07640.412 8929.62310.73-.007264     0 5 2     1 3 0  4  3  2    4  4  1   13223042322571 2 0    27.0   27.0
11 6503.559400 1.871E-65 2.548E-01.01270.08621151.86110.410.000000    -2-2-2    -2-2-2 30 -4 -4   29 -3 -3   13223042329171 2 0   183.0  177.0
```

Fig. 4. A sample extract from the new HITEMP water file. The parameters and columns are defined in Table 1. The transition in bold font is the line for which the frequency is taken from SELP. The transition in bold italic font is taken from HITRAN2008.

Since publication of the paper by Tashkun et al. [44], a number of new measurements of CO_2 line positions and intensities have been published. In 2008 an updated version of the CDSD databank called CDSD-1000 [49] was created. This version is considered as an improved and extended list with respect to the 2003 version. The

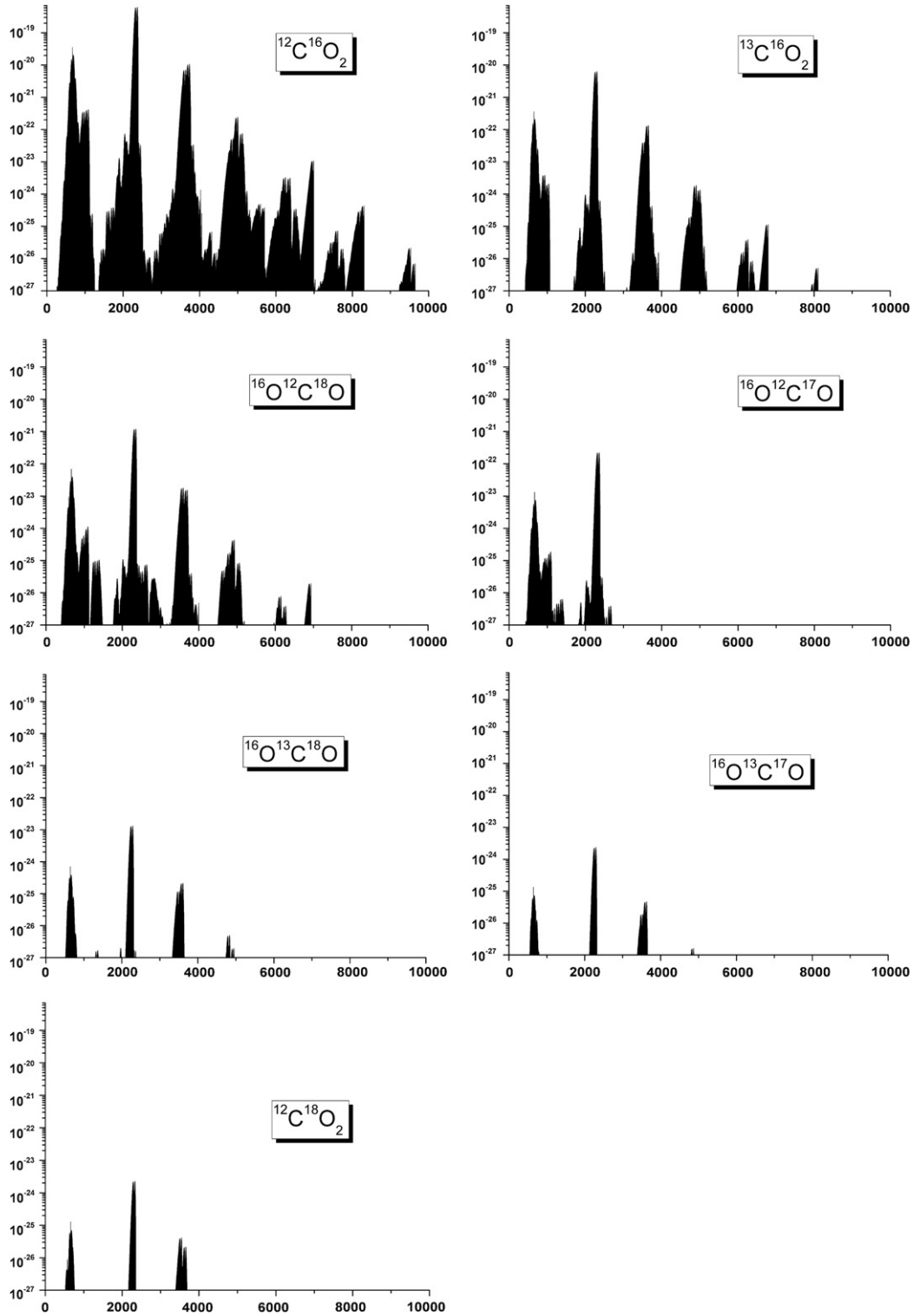

Fig. 5. Graphical overview of the CDSD-1000 databank [49]. All spectra are calculated at T_{ref}=1000 K. The *X* axis is in wavenumber (cm^{-1}) and the *Y* axis in intensity in HITRAN units (cm $molecule^{-1}$).

principal improvement is inclusion of $^{13}CO_2$ data in the range 3080–8100 cm^{-1}. In addition, data of three less abundant isotopologues, $^{16}O^{13}C^{18}O$, $^{16}O^{13}C^{17}O$, and $^{12}C^{18}O_2$, were added. This version follows the HITRAN2004 [14] format and is freely available via the Internet site ftp.iao.ru/pub/CDSD-2008/1000. A new version of CDSD, having T_{ref}=4000 K and an intensity cutoff of 10^{-27} cm $molecule^{-1}$, is under development.

The HITEMP2010 CO_2 parameters were calculated from CDSD-1000 parameters by rescaling intensities from T=1000 to T=296 K. The TIPS-2003 code supplied with the HITRAN compilation was used to calculate total internal partition sums. A graphical overview of the HITEMP2010 CO_2 is presented in Fig. 5.

In order to illustrate the quality of CDSD-1000, we performed simulations of a high-temperature emission spectrum given in Fig. 3 of Ludwig et al. [50]. The experimental conditions were T=1950 K, pressure=1 atm, geometrical path=3.12 cm, and slit width=5 cm^{-1}. The experimental curve of Ref. [50] was digitized. Results of the simulation using HITEMP1995 and CDSD-1000 are given in Fig. 6. It is seen that in the 500–700 cm^{-1} spectral interval both databanks give practically the same emissivity values. In the 700–850 cm^{-1} interval the CDSD-1000 simulation is closer to the observed curve than the HITEMP1995 one.

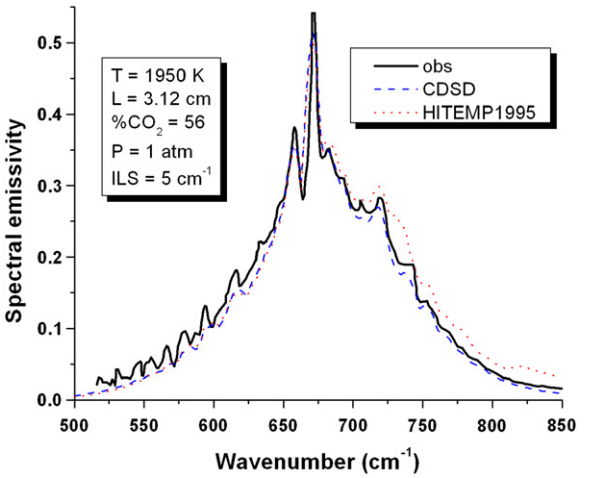

Fig. 6. Comparison of synthetic emission generated using CDSD-1000 [49] (dashed line) and HITEMP1995 [5] (dotted line) with high-temperature observations (solid line) given in Fig. 3 of Ref. [50]. The temperature is 1950 K, the total pressure is 1 atm, the geometrical path is 3.12 cm, and the slit width is 5 cm^{-1}.

3.3. CO

The line list for carbon monoxide that has been available in HITEMP1995 was retained for this new edition of HITEMP2010. The data were assembled from the solar atlas of Goorvitch [9]. The only exception is where there have been updates to the line parameters in HITRAN for carbon monoxide after 1995; in these cases the improved values were adopted for the HITEMP2010 compilation.

3.4. NO

The nitric oxide $X^2\Pi \leftarrow X^2\Pi$ line parameters included in HITEMP2010 are described in Goldman et al. [51,52]. These consist of the $^{14}N^{16}O$ transitions for Δv=0, …, 5 with v'=0, …, 14, and J_{max}=125.5. The Hamiltonian constants of Coudert et al. [53] were used for the rovibrational energy levels of v=0,1,2 taking into account Λ-doubling but not hyperfine structure. For the remaining bands, the Hamiltonian constants of Amiot [54] were used. The calculations for high v, J involved significant extrapolation beyond the available spectral measurements [52].

The line intensities were derived from wave functions and electric dipole-moment functions (EDMF). The wavefunction calculations were developed by Goorvitch and Galant [55,56] and by Chackerian et al. [57]. A combination of experimental EDMF by Spencer et al. [58] and theoretical EDMF by Langhoff et al. [59] and Holtzclaw et al. [60] was used.

For future work, it is important to address errors in terms of values identified for high v, J [51,52], and add various isotopologues of NO to the compilation.

3.5. OH

The $^{16}O^1H$ line parameters in HITEMP1995 were those generated by Goldman et al. [10], for the $X^2\Pi \leftarrow X^2\Pi$ transitions of Δv=0, …, 6 with v'=0, …, 10 and J_{max}=49.5. The line positions were calculated by combining and extending the studies of Abrams et al. [61], Mélen et al. [62], Coxon [63], and Coxon and Foster [64]. The line intensities were calculated from a composite of Nelson et al. [65] and Chackerian et al. [57] EDMF.

In subsequent studies, by Cosby et al. [66] and by Colin et al. [67], it was found that some of the spectroscopic constants used by Goldman et al. [10] led to errors at higher vibrational ($v > 3$) and rotational ($J > 19.5$) levels, producing differences with experiment up to 0.14 cm^{-1}. Recently, Bernath and Colin [68] reanalyzed all the published experimental data for the electronic ground state of the hydroxyl radical, to which they added transitions determined from their solar spectrum [68]. They produced a new set of term values for v=0, …, 10, extrapolated to five J values above the last observed one.

These results were used to revise all the OH transitions (where hyperfine structure was not resolved) in the HITRAN database with updated positions and ground-state energy values, and the same was performed for the new HITEMP database. Note that line positions in HITEMP of the transitions beyond those kept for HITRAN are not validated.

The intensities have not been updated in this current effort. Recently, van der Loo and Groenenboom [69,70] used ab initio calculations to generate a new potential energy curve, electric dipole-moment function, and spin-orbit coupling function for the OH $X^2\Pi$ state. These functions were used to compute a new set of Einstein A-coefficients. In a future update of the $^{16}O^1H$ line parameters for HITEMP (and HITRAN) the new Einstein

A-coefficients [70] may be utilized after validation. Also, more data on the isotopologues of OH should be added to the compilation.

4. Computation of highly excited molecular spectra

HITEMP continues to be an extremely useful database for many applications requiring the prediction of spectral signatures from highly excited vibrational levels, for example at high altitudes where NLTE conditions prevail, in auroral events, or in rocket plume simulations. Under these conditions, vibrational bands are described by their own vibrational temperatures, which deviate from the local temperature. Current NLTE models, such as SAMM2 [71] predict line strengths by calculating the population ratio and combining it with the square of the transition moments, which can be easily derived from the HITEMP data, as described in Gamache and Rothman [72].

Recently a semiclassical approach has been employed by Dothe et al. [73] to compute high-temperature absorption cross-sections that in the future can supplement HITEMP data where line lists are not readily available. The approach, dubbed CHEMS (Computation of Highly Excited Molecular Spectra), exploits the fact that in the high-temperature limit, rotational lines blend together to form a smooth cross-section envelope that can be described at a lower spectral resolution. The method is based on evaluating the Fourier Transform of the time correlation function of the dipole moment of the vibrating–rotating molecule for normal mode trajectories that satisfy semiclassical quantization conditions as described by Schatz [74]. The CHEMS approach was developed to obtain high-temperature absorption cross-sections required to model plume signatures, when existing databases of such cross-sections are incomplete, inaccurate, or not available at sufficiently high temperatures. It is currently being tested in application to CO_2, H_2O, and NH_3 molecules that are important in hot plume signatures.

5. Conclusion

A new edition of the high-temperature molecular absorption database, HITEMP2010, has been constructed. This edition includes molecular transitions for five species: H_2O, CO_2, CO, NO, and OH. Table 4 summarizes the spectral coverage of the new edition, and shows a comparison to the standard atmospheric database, HITRAN, in terms of size. The last column presents the dissociation energies of the molecules.

The structure of the database remains the same as the HITRAN database, but it is expected that this structure will be modernized in the near future, most likely following relational database schemes. One such scheme that is being investigated is part of the information system being developed by the water-vapor task group of IUPAC [34].

There are many applications for a high-temperature molecular spectroscopic database. It is obviously necessary to include more molecular species. We anticipate adding NO^+, hydrogen halides, N_2O, CH_4, NH_3, and C_2H_2, for example. However, the challenges are myriad, both from the experimental and theoretical sides.

One of the most important additions to HITEMP would be methane. There exists a substantial effort at the University of Burgundy called spherical top data system (STDS) [80] to generate high-resolution spectra of lower polyads at high temperature (2000 K). Perrin and Soufiani [81] used the STDS software and used a statistical approach for hot bands, i.e., create low resolution data for them.

Ongoing efforts for obtaining absorption parameters of methane at elevated temperatures, include the work of Boudon [82] to generate better spectra of lower polyads at high temperature (2000 K) by updating the STD software [83] and obtaining the best available input parameters for it. Meanwhile, a new ab initio potential-energy surface has appeared [84] and will be studied towards its potential application to HITEMP.

In the future we hope to add a high-temperature line list for the ammonia molecule. Recently Yurchenko et al. [85] computed a low-temperature line list; a hot line list with improved accuracy is currently being produced.

Instructions for access to the databases can be found on the web site at http://www.cfa.harvard.edu/HITRAN.

Acknowledgments

We acknowledge the support of NASA through the Earth Observing System (EOS) program under the Grant no. NAG5-13534 and the Planetary Atmospheres program under Grant no. NNX10AB94G. We also acknowledge the CHEMS (Computation of Highly Excited Molecular

Table 4
Line list comparison between HITEMP2010 and HITRAN [2].

Molecule	Spectral coverage (cm^{-1})	Number of isotopologues[a] (HITEMP2010)	Number of transitions (HITEMP2010)	Number of transitions[b] (HITRAN)	Dissociation energy (cm^{-1})
H_2O	0–30,000	6	111,377,777	69,201	41,145.94 ± 0.15 [75]
CO_2	258–9648	7	11,167,618	312,479	44,360 [76]
CO	0–8465	6	115,218	4,477	90,674 ± 15 [77]
NO	0–9274	3	105 633	105,079	52,265 [78]
OH	0–19,268	3	40,055	31,976	35,593 ± 25 [79]

[a] For H_2O, NO, and OH, only the principal isotopologue has been created for high temperature at this time. The other lesser abundant isotopologues have been transcribed from HITRAN (296 K).
[b] The number of transitions listed in this column are for the equivalent number of isotopologues and spectral range consistent with HITEMP2010.

Spectra) SBIR project through Spectral Sciences, Inc. RRG acknowledges support of this research by the National Science Foundation through Grant no. ATM-0803135. VIP and SAT acknowledge support by the Russian Fund of Basic Research under the Grant nos. 06-05-39016-ГФЕН_а and 09-05-93105-НЦНИЛ_а.

References

[1] McClatchey RA, Benedict WS, Clough SA, Burch DE, Calfee RF, Fox K, et al. AFCRL atmospheric absorption line parameters compilation. AFCRL-technical report-0096, 1973.
[2] Rothman LS, Gordon IE, Barbe A, Benner DC, Bernath PF, Birk M, et al. The HITRAN 2008 molecular spectroscopic database. J Quant Spectrosc Radiat Transfer 2009;110:533–72.
[3] Tinetti G, Vidal-Madjar A, Liang M-C, Beaulieu J-P, Yung Y, Carey S, et al. Water vapour in the atmosphere of a transiting extrasolar planet. Nature 2007;448:169–71.
[4] Barber RJ, Tennyson J, Harris GJ, Tolchenov RN. A high-accuracy computed water line list. Mon Not R Astron Soc 2006;368: 1087–94.
[5] Rothman LS, Wattson RB, Gamache RR, Schroeder J, McCann A. HITRAN, HAWKS and HITEMP high-temperature molecular database. Proc Soc Photo-Opt Instrum Eng 1995;2471:105–11.
[6] Pollack JB, Dalton JB, Grinspoon D, Wattson RB, Freedman R, Crisp D, et al. Near-infrared light from Venus' nightside: a spectroscopic analysis. Icarus 1993;103:1–42.
[7] Meinel IAB. OH emission bands in the spectrum of the night sky. Astrophys J 1950;111:555–64.
[8] Wattson RB, Rothman LS. Direct numerical diagonalization: wave of the future. J Quant Spectrosc Radiat Transfer 1992;48:763–80.
[9] Goorvitch D. Infrared CO line list for the $X^1\Sigma^+$ state. Astrophys J Suppl Ser 1994;95:535–52.
[10] Goldman A, Schoenfeld WG, Goorvitch D, Chackerian Jr. C, Dothe H, Mélen F, et al. Updated line parameters for OH $X^2\Pi$—$X^2\Pi$ (v'',v') transitions. J Quant Spectrosc Radiat Transfer 1998;59: 453–69.
[11] Rothman LS, Gamache RR, Tipping RH, Rinsland CP, Smith MAH, Benner DC, et al. The HITRAN molecular database—editions of 1991 and 1992. J Quant Spectrosc Radiat Transfer 1992;48: 469–507.
[12] Gordon IE, Dothe H, Rothman LS. The resurrection of the HITEMP database and its application to the study of stellar and planetary atmospheres. European Geosciences Union General Assembly, Vienna, Austria, 2007.
[13] Rothman LS, Gamache RR, Goldman A, Brown LR, Toth RA, Pickett HM, et al. The HITRAN database—1986 edition. Appl Opt 1987;26: 4058–97.
[14] Rothman LS, Jacquemart D, Barbe A, Chris Benner D, Birk M, Brown LR, et al. The HITRAN 2004 molecular spectroscopic database. J Quant Spectrosc Radiat Transfer 2005;96:139–204.
[15] Simecková M, Jacquemart D, Rothman LS, Gamache RR, Goldman A. Einstein *A*-coefficients and statistical weights for molecular absorption transitions in the HITRAN database. J Quant Spectrosc Radiat Transfer 2006;98:130–55.
[16] Partridge H, Schwenke DW. The determination of an accurate isotope dependent potential energy surface for water from extensive ab initio calculations and experimental data. J Chem Phys 1997;106:4618–39.
[17] Schwenke DW, Partridge H. Convergence testing of the analytic representation of an ab initio dipole moment function for water: improved fitting yields improved intensities. J Chem Phys 2000;113:6592–7.
[18] Jørgensen UG, Jensen P, Sørensen GO, Aringer B. H_2O in stellar atmospheres. Astron Astrophys 2001;372:249–59.
[19] Jensen P. The potential energy surface for the electronic ground state of the water molecule determined from experimental data using a variational approach. J Mol Spectrosc 1989;133:438–60.
[20] Jørgensen UG, Jensen P. The dipole moment surface and the vibrational transition moments of H_2O. J Mol Spectrosc 1993;161: 219–42.
[21] Shirin SV, Polyansky OL, Zobov NF, Barletta P, Tennyson J. Spectroscopically determined potential energy surface of $H_2^{16}O$ up to 25,000 cm^{-1}. J Chem Phys 2003;118:2124–9.
[22] Campargue A, Mikhailenko SN, Liu AW. ICLAS of water in the 770 nm transparency window (12,746–13,558 cm^{-1}). Comparison with current experimental and calculated databases. J Quant Spectrosc Radiat Transfer 2008;109:2832–45.
[23] Bailey J. A comparison of water vapor line parameters for modeling the Venus deep atmosphere. Icarus 2009;201:444–53.
[24] Kranendonk LA, An X, Caswell AW, Herold RE, Sanders ST, Huber R, et al. High speed engine gas thermometry by Fourier-domain mode-locked laser absorption spectroscopy. Opt Express 2007;15: 15115–28.
[25] Coppalle A, Vervisch P. Spectral emissivities of H_2O vapor at 2900 K in the 1–9-μm region. J Quant Spectrosc Radiat Transfer 1986;35: 121–5.
[26] Barber RJ, Miller S, Dello Russo N, Mumma MJ, Tennyson J, Guio P. Water in the near-infrared spectrum of comet 8P/Tuttle. Mon Not R Astron Soc 2009;398:1593–600.
[27] Sharp CM, Burrows A. Atomic and molecular opacities for brown dwarf and giant planet atmospheres. Astrophys J Suppl Ser 2007; 168:140–66.
[28] Perez P, Boischot A, Ibgui L, Roblin A. A spectroscopic database for water vapor adapted to spectral properties at high temperature, and moderate resolution. J Quant Spectrosc Radiat Transfer 2007;103:231–44.
[29] Voronin BA, Tennyson J, Tolchenov RN, Lugovskoy AA, Yurchenko SN. A high accuracy computed line list for the HDO molecule. Mon Not R Astron Soc 2010;402:492–6.
[30] Tennyson J, Zobov NF, Williamson R, Polyansky OL, Bernath PF. Experimental energy levels of the water molecule. J Phys Chem Ref Data 2001;30:735–831.
[31] Zobov NF, Polyansky OL, Tennyson J, Shirin SV, Nassar R, Hirao T, et al. Using laboratory spectroscopy to identify lines in the K- and L-band spectrum of water in a sunspot. Astrophys J 2000;530: 994–8.
[32] Coheur P-F, Bernath PF, Carleer M, Colin R, Polyansky OL, Zobov NF, et al. A 3000 K laboratory emission spectrum of water. J Chem Phys 2005;122:4307.
[33] Zobov NF, Shirin SV, Polyansky OL, Barber RJ, Tennyson J, Coheur P-Fo, et al. Spectrum of hot water in the 2000–4750 cm^{-1} frequency range. J Mol Spectrosc 2006;237:115–22.
[34] Tennyson J, Bernath PF, Brown LR, Campargue A, Carleer MR, Császár AG, et al. IUPAC critical evaluation of the rotational–vibrational spectra of water vapor. Part I—energy levels and transition wavenumbers for $H_2^{17}O$ and $H_2^{18}O$. J Quant Spectrosc Radiat Transfer 2009;110:573–96.
[35] Gordon IE, Rothman LS, Gamache RR, Jacquemart D, Boone C, Bernath PF, et al. Current updates of the water-vapor line list in HITRAN: a new "diet" for air-broadened half-widths. J Quant Spectrosc Radiat Transfer 2007;108:389–402.
[36] Jacquemart D, Gamache R, Rothman LS. Semi-empirical calculation of air-broadened half-widths and air pressure-induced frequency shifts of water-vapor absorption lines. J Quant Spectrosc Radiat Transfer 2005;96:205–39.
[37] Gamache RR, Hartmann JM. An intercomparison of measured pressure-broadening and pressure-shifting parameters of water vapor. Can J Chem 2004;82:1013–27.
[38] Gamache RR, Laraia AL. N_2-, O_2-, and air-broadened half-widths, their temperature dependence, and line shifts for the rotation band of $H_2^{16}O$. J Mol Spectrosc 2009;257:116–27.
[39] Gamache RR. Lineshape parameters for water vapor in the 3.2–17.76 μm region for atmospheric applications. J Mol Spectrosc 2005;229:9–18.
[40] Wagner G, Birk M, Gamache RR, Hartmann J-M. Collisional parameters of H_2O lines: effect of temperature. J Quant Spectrosc Radiat Transfer 2005;92:211–30.
[41] Toth RA, Brown LR, Smith MAH, Malathy Devi V, Chris Benner D, Dulick M. Air-broadening of H_2O as a function of temperature: 696–2163 cm^{-1}. J Quant Spectrosc Radiat Transfer 2006;101: 339–66.
[42] Vidler M, Tennyson J. Accurate partition function and thermodynamic data for water. J Chem Phys 2000;113:9766–71.
[43] Tashkun SA, Perevalov VI, Teffo JL, Bykov AD, Lavrentieva NN. CDSD-296, the carbon dioxide spectroscopic databank: version for atmospheric applications. In: XIVth symposium on high resolution molecular spectroscopy. Krasnoyarsk, Russia, July 6–11; 2003. See also ⟨ftp://ftp.iao.ru/pub/CDSD-296/⟩.
[44] Tashkun SA, Perevalov VI, Teffo JL, Bykov AD, Lavrentieva NN. CDSD-1000, the high-temperature carbon dioxide spectroscopic databank. J Quant Spectrosc Radiat Transfer 2003;82:165–96.
[45] Bharadwaj SP, Modest MF. Medium resolution transmission measurements of CO_2 at high temperature—an update. J Quant Spectrosc Radiat Transfer 2007;103:146–55.

[46] Modest MF, Mehta RS. Full spectrum *k*-distribution correlations for CO_2 from the CDSD-1000 spectroscopic databank. Int J Heat Mass Transfer 2004;47:2487–91.
[47] Wang A, Modest MF. High-accuracy, compact database of narrow-band *k*-distributions for water vapor and carbon dioxide. J Quant Spectrosc Radiat Transfer 2007;93:245–61.
[48] Bharadwaj SP, Modest MF. A multiscale Malkmus model for treatment of inhomogeneous gas paths. Int J Therm Sci 2007;46: 479–90.
[49] Tashkun SA, Perevalov VI. CDSD (carbon dioxide spectroscopic databank): updated and enlarged version for atmospheric applications. Paper T2.3, tenth HITRAN conference. Cambridge MA; 2008. See also ⟨ftp://ftp.iao.ru/pub/CDSD-2008/⟩.
[50] Ludwig CB, Ferriso CC, Acton L. High-temperatures spectral emissivities and total intensities of the 15-μm band system of CO_2. J Opt Soc Am 1966;56:1685–92.
[51] Goldman A Updated line parameters for NO $X\ ^2\Pi$—$X\ ^2\Pi$ (v'', v'). Progress report. University of Denver, December 27; 1996.
[52] Goldman A, Brown LR, Schoenfeld WG, Spencer MN, Chackerian Jr. C, Giver LP, et al. Nitric oxide line parameters: review of 1996 HITRAN update and new results. J Quant Spectrosc Radiat Transfer 1998;60:825–38.
[53] Coudert LH, Dana V, Mandin JY, Morillon-Chapey M, Farrenq R. The spectrum of nitric oxide between 1700 and 2100 cm^{-1}. J Mol Spectrosc 1995;172:435–48.
[54] Amiot C. The infrared emission spectrum of NO: analysis of the $\Delta v=0$ sequence up to $v=22$. J Mol Spectrosc 1982;94:150–72.
[55] Goorvitch D, Galant DC. Schrödinger's radial equation: solution by extrapolation. J Quant Spectrosc Radiat Transfer 1992;47:391–9.
[56] Goorvitch D, Galant DC. The solution of coupled Schrödinger equations using an extrapolation method. J Quant Spectrosc Radiat Transfer 1992;47:505–13.
[57] Chackerian C, Goorvitch D, Benidar A, Farreno R, Guelachvili G, Martin PM, et al. Rovibrational intensities and electric dipole moment function of the $X^2\Pi_i$ hydroxyl radical. J Quant Spectrosc Radiat Transfer 1992;48:667–73.
[58] Spencer MN, Chackerian C, Giver LP, Brown LR. The Nitric oxide fundamental band: frequency and shape parameters for rovibrational lines. J Mol Spectrosc 1994;165:506–24.
[59] Langhoff Jr. SR, W BC, Partidge H. Theoretical dipole moment for the $X^2\Pi$ state of NO. Chem Phys Lett 1994;223:416–22.
[60] Holtzclaw KW, Rawlins WT, Green BD. The effects of centrifugal distortion on the infrared radiative transition probabilities of NO($X^2\Pi$). J Quant Spectrosc Radiat Transfer 1996;55:481–92.
[61] Abrams MC, Davis SP, Rao MLP, Engleman RJ, Brault JW. High-resolution Fourier transform spectroscopy of the Meinel system of OH. Astrophys J Suppl Ser 1994;93:351–95.
[62] Mélen F, Sauval AJ, Grevesse N, Farmer CB, Servais C, Delbouille L, et al. A new analysis of the OH radical spectrum from solar infrared observations. J Mol Spectrosc 1995;174:490–509.
[63] Coxon JA. Optimum molecular constants and term values for the $X^2\Pi$ ($v \le 5$) and $A^2\Sigma^+$ ($v \le 3$) states of OH. Can J Phys 1980;58: 933–49.
[64] Coxon JA, Foster AC. Rotational analysis of hydroxyl vibration–rotation emission bands: molecular constants for OH $X^2\Pi$, $6 \le v \le 10$. Can J Phys 1982;60:41–8.
[65] Nelson Jr. DD, Schiffman A, Nesbitt DJ, Orlando JJ, Burkholder JBH. O_3 Fourier transform infrared emission and laser absorption of OH ($X^2\Pi$) radical: an experimental dipole moment function and state-to-state Einstein *A* coefficients. J Chem Phys 1990;93:7003–19.
[66] Cosby PC, Slanger TG, Huestis DL, Ostenbrock DE. Term energies, line positions, and spectroscopic constants for the OH Meinel band system. In: The 55th Ohio State University International Symposium on Molecular Spectroscopy, 2000. ⟨http://spectroscopy.mps.ohio-state.edu/symposium_55/symposium/Program/TA.html#TA-01⟩.
[67] Colin R, Coheur P-F, Kiseleva M, Vandaele AC, Bernath PF. Spectroscopic constants and term values for the $X^2\Pi_i$ state of OH ($v=0$–10). J Mol Spectrosc 2002;214:225–6.
[68] Bernath PF, Colin R. Revised molecular constants and term values for the $X^2\Pi_i$ and B^2S^+ states of OH. J Mol Spectrosc 2009;257:20–3.
[69] van der Loo MPJ, Groenenboom GC. Theoretical transition probabilities for the OH Meinel system. J Chem Phys 2007;126: 4314.
[70] van der Loo MPJ, Groenenboom GC. Erratum: "theoretical transition probabilities for the OH Meinel system" [J Chem Phys 126, 114314 (2007)]. J Chem Phys 2008;128:9902.
[71] Dothe H, Duff JW, Gruninger JH, Acharya PK, Berk A, Brown JH. Users' manual for SAMM2, SHARC-4 and MODTRAN-4 merged. Report: AFRL-VS-HA-TR-2004-1001. 2004.
[72] Gamache RR, Rothman LS. Extension of the HITRAN database to non-LTE applications. J Quant Spectrosc Radiat Transfer 1992;48: 519–25.
[73] Dothe H, Duff JW, Rothman LS, Gordon I. Computation of highly excited molecular spectra (CHEMS). In: The 19th international conference on high resolution infrared spectroscopy. Prague, Czech Republic; 2006.
[74] Schatz GCA. Program for determining primitive semiclassical eigenvalues for vibrating/rotating nonlinear triatomic molecules. Comput Phys Commun 1988;51:135.
[75] Matsyutenko P, Rizzo TR, Boyarkin OV. A direct measurement of the dissociation energy of water. J Chem Phys 2006;125: 181101.
[76] Davies WO. Carbon dioxide dissociation at 6000° to 11,000 °K. J Chem Phys 1965;43:2809–18.
[77] Eidelsberg M, Roncin J-Y, Le Floch A, Launay F, Letzelter C, Rostas J. Reinvestigation of the vacuum ultraviolet spectrum of CO and isotopic species: the $B^1\Sigma^+ \leftrightarrow X^1\Sigma^+$ transition. J Mol Spectrosc 1987; 121:309–36.
[78] Brook M, Kaplan J. Dissociation energy of NO and N_2. Phys Rev 1954;96:1540–2.
[79] Ruscic B, Wagner AF, Harding LB, Asher RL, Feller D, Dixon DA, et al. On the enthalpy of formation of hydroxyl radical and gas-phase bond dissociation energies of water and hydroxyl. J Phys Chem A 2002;106:2727–47.
[80] Wenger C, Champion JP, Boudon V. The partition sum of methane at high temperature. J Quant Spectrosc Radiat Transfer 2008;109: 2697–706.
[81] Perrin M-Y, Soufiani A. Approximate radiative properties of methane at high temperature. J Quant Spectrosc Radiat Transfer 2007;103:3–13.
[82] Boudon V. University of Burgundy, Private Communication, 2008.
[83] Wenger Ch, Boudon V, Champion JP, Pierre G. Highly-spherical top data system (HTDS) software for the spectrum simulation of octahedral XY_6 molecules. J Quant Spectrosc Radiat Transfer 2000;66(1):1–16 See also: ⟨http://icb.u-bourgogne.fr/OMR/SMA/SHTDS⟩.
[84] Warmbier R, Schneider R, Sharma AR, Braams BJ, Bowman JM, Hauschildt PH. Ab initio modeling of molecular IR spectra of astrophysical interest: application to CH_4. Astron Astrophys 2009;495:655–61.
[85] Yurchenko SN, Barber RJ, Yachmenev A, Theil W, Jensen P, Tennyson J. A variationally computed $T=300$ K line list for NH_3. J Phys Chem A 2009;113:11845–55.